International Journal of Heat and Technology
Vol. 44, No. 4, August, 2026, pp. 1483-1493
Journal homepage: http://iieta.org/journals/ijht

Thermally-Assisted Synthesis of La-Zeolite for Low-Level Phosphorus Remediation in Estuarine Rivers: Adsorption Thermodynamics and Mechanisms

Meng Wang[1], Haibo Lun[1], Zunju Zhang[2], Yarong Dong[1], Lei Sun[1], Na Sun[3], Jing Li[3*]

[1] Center for Research and Experimental Technology on Environment, Hebei University of Environmental Engineering, Qinhuangdao 066100, China
[2] Department of Environmental Engineering, Hebei University of Environmental Engineering, Qinhuangdao 066100, China
[3] Research Office, Hebei University of Environmental Engineering, Qinhuangdao 066100, China

Corresponding Author Email: lijing@hebuee.edu.cn

Copyright: ©2026 The authors. This article is published by IIETA and is licensed under the CC BY 4.0 license (http://creativecommons.org/licenses/by/4.0/).

https://doi.org/10.18280/ijht.440413

Received: 10 April 2026
Revised: 17 August 2026
Accepted: 25 August 2026
Available online: 31 August 2026

Keywords:
thermally-assisted modification, lanthanum-modified zeolite, adsorption thermodynamics, rivers discharging into the sea, low-phosphorus remediation

ABSTRACT

To address the technical demands for controlling low-concentration phosphorus pollution in rivers discharging into the sea, this study employed a thermally-assisted impregnation method to prepare lanthanum nitrate-modified clinoptilolite. The effects of heat treatment conditions (temperature and time) during preparation on the material's microstructure and phosphorus removal performance were systematically investigated, with a particular focus on revealing the thermodynamic behavior of the adsorption process. Characterization via Scanning Electron Microscopy (SEM)–Energy Dispersive Spectroscopy (EDS), Brunauer–Emmett–Teller (BET), and X-ray Diffraction (XRD) demonstrated that heat treatment promoted the uniform loading of lanthanum hydrate onto the zeolite surface and constructed a hierarchical micro-mesoporous skeleton structure, effectively reducing the internal diffusion mass transfer resistance of phosphate ions. Adsorption thermodynamics and kinetic fitting results showed that the Langmuir model ($R^2 = 0.9834$) and the pseudo-second-order kinetic model ($R^2 = 0.9961$) provided the best fit. The theoretical maximum adsorption capacity reached 7.94 mg/g, representing an approximately eightfold increase compared to natural zeolite. Temperature effect experiments indicated that the removal rate remained stable at 85%–89% within the range of 20–40 °C. However, excessively high temperatures (>40 °C) disrupted the lanthanum hydration structure and complex stability, manifesting as an exothermic adsorption characteristic. Activation energy and thermodynamic parameters (ΔG^0, ΔH^0, ΔS^0) calculated based on the Arrhenius and van 't Hoff equations further confirmed that the adsorption process is a spontaneous, exothermic, monolayer reaction dominated by chemical coordination. Validation using actual water from six rivers in Qinhuangdao showed that the average removal rate in static adsorption reached 73.3%, with all effluent total phosphorus concentrations meeting the Surface Water Class III standard (≤0.2 mg/L). In dynamic fixed-bed continuous flow tests, the removal rate remained stable above 75% under low load fluctuations. This study demonstrates that thermally-assisted lanthanum modification, through a triple mechanism of enhancing chemical driving force, introducing phosphate-specific recognition sites, and optimizing pore structure, endows the material with excellent adsorption capacity, rapid adsorption kinetics, and good temperature adaptability. This provides thermodynamic theoretical support and engineering technical references for the treatment of low-phosphorus pollution in rivers discharging into the sea.

1. INTRODUCTION

Phosphorus is a key limiting factor for eutrophication in surface water bodies, and excessive total phosphorus poses threats to regional ecological balance and drinking water safety [1]. In Qinhuangdao, the Shihe River, Daihe River, Yanghe River, etc., under the combined effects of non-point source pollution and industrial and domestic wastewater, excessive total phosphorus has become a key challenge in local water environment management [2].

Zeolite is regarded as an ideal adsorbent due to its abundant reserves, low cost, and good pore structure [3]. However, the selectivity and capacity of natural zeolite for phosphorus removal are relatively limited, which restricts its large-scale application [4]. In view of the strong specific affinity between lanthanum and phosphate, enhancing the phosphorus immobilization capacity of zeolite through lanthanum modification has become an important direction in water treatment research both domestically and internationally. Luo et al. [5] used a co-precipitation-hydrothermal method to fabricate Lanthanum-modified natural Zeolite (LZ) and Lanthanum-modified Magnetic Zeolite (LMZ). The study showed that the phosphorus saturation adsorption capacities of LZ and LMZ reached 122.7 mg/g and 109.17 mg/g,

respectively. Chen et al. [6] applied lanthanum modification technology to the field of fly ash synthetic zeolite, creating a new application for material resource utilization. After lanthanum series elements were loaded onto the pore size and surface interface of synthetic zeolite, the phosphorus removal efficiency increased significantly from less than 30% to 94.2%, with a performance improvement of approximately 65%.

Currently, lanthanum-modified zeolites are mostly prepared by co-precipitation, hydrothermal treatment, or direct impregnation. Co-precipitation and hydrothermal methods may suffer from high energy consumption, uneven La distribution, and pore blockage, whereas direct impregnation often leads to limited La binding strength and easy La leaching. Heat-assisted impregnation can regulate the hydrolysis and polymerization of La and its interfacial binding with the support through thermal treatment; however, the relationship among heat-treatment conditions, structure, and low-phosphorus adsorption thermodynamics remains unclear. Existing studies have mostly focused on high-concentration phosphorus or sediment passivation, and systematic studies on low total phosphorus (TP ≤ 0.5 mg/L) in rivers entering the sea, with effluent meeting the Class III surface water standard (≤ 0.2 mg/L), are still insufficient. In particular, validation using actual water bodies and dynamic continuous-flow systems is lacking.

This study takes natural clinoptilolite as the substrate to optimize the lanthanum modification preparation process. Scanning Electron Microscopy (SEM)–Energy Dispersive Spectroscopy (EDS), Brunauer–Emmett–Teller (BET), X-ray Diffraction (XRD), and other means are used to characterize the microstructural evolution of zeolite before and after modification. Combined with adsorption isotherms and kinetic models, the adsorption performance is systematically compared, the selective adsorption mechanism is revealed, the influence of key environmental factors is explored, and the characteristics of low-concentration phosphorus pollution (mass concentration ≤ 0.5 mg/L) in rivers discharging into the sea are directionally adapted. On this basis, the modified material is applied to the actual water bodies of typical rivers discharging into the sea in Qinhuangdao. Static and dynamic adsorption tests are carried out in combination with actual raw water from rivers discharging into the sea to evaluate its in-situ remediation prospects.

2. MATERIALS AND METHODS

2.1 Preparation of modified zeolite

The zeolite was rinsed three times with distilled water until the wash water became clear, dried at 60–80 ℃ for 1 h, and stored in a sealed container. The pretreated zeolite was immersed in a 10 g/L lanthanum nitrate solution at pH 11, shaken at 25 ℃ and 150 r/min for 10 h, and then placed in a muffle furnace. Under an air atmosphere, the sample was heated at a rate of 5 ℃/min to 300 ℃, held for 2 h, naturally cooled to room temperature, and stored in a sealed container [7-9].

2.2 Characterization analysis of modified zeolite

SEM was used to observe the surface morphology of zeolite before and after modification and analyze the elemental composition. Before testing, the samples mounted on conductive adhesive were gold-sprayed for conductivity enhancement. A physical adsorption instrument was used to measure the N_2 adsorption-desorption isotherms at 77.3 K to obtain the specific surface area, pore volume, and pore size distribution. XRD was used to analyze the phase composition and crystallization characteristics. The test conditions were set as Cu target, voltage 40 kV, current 40 mA, continuous scanning at a speed of 10°/min in the range of 5°–90°, and the sampling step width was set to 0.01719°.

2.3 Adsorption mechanism and kinetic analysis of modified zeolite

Langmuir and Freundlich models were used to fit the isothermal adsorption data [10, 11]. The Langmuir model assumes monolayer adsorption on a homogeneous surface, where all active sites have the same energy, and the rates of adsorption and desorption are equal at equilibrium until adsorption saturation is reached. The Freundlich model is used to describe adsorption on heterogeneous interfaces.

Pseudo-first-order and pseudo-second-order kinetic models were used to fit the adsorption rate data. The pseudo-first-order model uses concentration gradient as the driving force, and the pseudo-second-order model involves chemical bonding forces. Under actual working conditions, the adsorption rate is often jointly limited by multiple mechanisms [12-14], so it is not necessarily completely consistent with a single reaction rate model in theory.

$$C_e/q_e = C_e/q_m + 1/(q_m K_L) \quad (1)$$

$$\log q_e = (1/n)\log C_e + \log K_F \quad (2)$$

$$\log(q_e - q_t) = \log q_e - (k_f/2.303)t \quad (3)$$

$$t/q_t = 1/(k_s q_e^2 t) + t/q_e \quad (4)$$

where, C_e is the total phosphorus mass concentration at adsorption equilibrium, mg/L; q_e is the equilibrium adsorption capacity, mg/g; K_L is the Langmuir isotherm coefficient; K_F is the Freundlich isotherm coefficient; 1/n is the adsorption constant.

2.4 Adsorption experiment design of modified zeolite

La-modified zeolite mainly adsorbs orthophosphate; TP serves as an apparent indicator, while organic phosphorus and particulate phosphorus need to be pre-converted. Static batch experiments were used to study the phosphorus adsorption performance of the modified zeolite and analyze its thermodynamic and kinetic mechanisms. After adsorption saturation, the mixture was allowed to stand for 30 min, and the supernatant was taken and measured at 720 nm by the ammonium molybdate spectrophotometric method according to GB 11893 [15]. Process parameters were optimized by the single-factor method, as shown in Table 1.

2.5 Desorption performance and reuse stability experiments

The experimental design scheme for analyzing performance and reuse stability performance is shown in Table 2, including three parts: desorbent screening, evaluation of adsorption

performance after regeneration, and multiple-cycle stability tests.

2.6 Actual water validation experiments

To investigate the phosphorus removal performance of the modified zeolite in natural water bodies, six rivers discharging into the sea in Qinhuangdao City—the Shihe River, Tanghe River, Daihe River, Yanghe River, Yinma River, and Xinhe River—were selected as the experimental raw water. After sampling, the water samples were stored at low temperature and protected from light, transported back to the laboratory within 24 h, and allowed to settle naturally for 1–2 h to remove large particles. The supernatant was vacuum-filtered through a 0.45 μm filter membrane. The Yanghe River and Yinma River water samples were pre-oxidized with $Na_2S_2O_8$ to eliminate organic interference. The pretreated water samples were stored at 4 ℃, and static adsorption experiments were completed within 48 h.

Table 1. Experimental design for optimization of adsorption parameters

Research Factor	Fixed Parameters	Variation Levels
Initial solution pH	Initial mass concentration: 0.5 mg/L; particle size: 2–4 mm; temperature: 25 ℃; time: 1 h; dosage: 10 g/L	4, 6, 7, 8, 9
Zeolite particle size	Initial mass concentration: 0.5 mg/L; dosage: 10 g/L; temperature: 25 ℃; time: 1 h; pH: 9	1-2, 2-4, 4-6, 6-8, 8-10, 10-12, 12-14, 14-16 mm
Initial total phosphorus mass concentration	Dosage: 10 g/L; particle size: 2–4 mm; temperature: 25 ℃; time: 1 h; pH: 9	0.2-1.0 mg/L
Zeolite dosage	Initial mass concentration: 0.5 mg/L; particle size: 2–4 mm; temperature: 25 ℃; time: 1 h; pH: 9	5, 10, 15, 20, 25 g/L
Reaction time	Dosage: 10 g/L; particle size: 2–4 mm; initial mass concentration: 0.5 mg/L; temperature: 25 ℃; pH: 9	15, 30, 60, 90, 120 min
Reaction temperature	Dosage: 10 g/L; particle size: 2–4 mm; initial mass concentration: 0.5 mg/L; time: 1 h; pH: 9	5, 10, 15, 20, 25, 30, 40, 50, 60 ℃

Table 2. Experimental design for desorption performance and reuse stability

Research Content	Experimental Method	Result Comparison
Desorbent screening	Take 10 g of phosphorus-saturated lanthanum nitrate modified zeolite and place it in 250 mL of NaOH, NaCl, and HCl solutions (concentrations: 3.0, 3.5, 4.0, 4.5 mol/L, respectively). Stir at room temperature for 3 h. Deionized water is used as the blank control.	Measure the phosphate concentration in the desorption solution and calculate the desorption rate (De).
Adsorption performance evaluation after regeneration	Filter, wash, and dry the desorbed zeolite. Conduct adsorption experiments under the same conditions (initial total phosphorus mass concentration 0.5 mg/L, dosage 10 g/L, 25 ℃, 150 r/min, 3 h).	Measure the removal rate after regeneration and the regeneration efficiency (η = Rr / raw material removal rate × 100%).
Multiple-cycle stability test	Using 4 mol/L NaOH as the regeneration solution, repeat the operation of "adsorption → desorption → washing → drying → re-adsorption".	Measure the removal rate of each cycle until the removal rate drops below 20%.

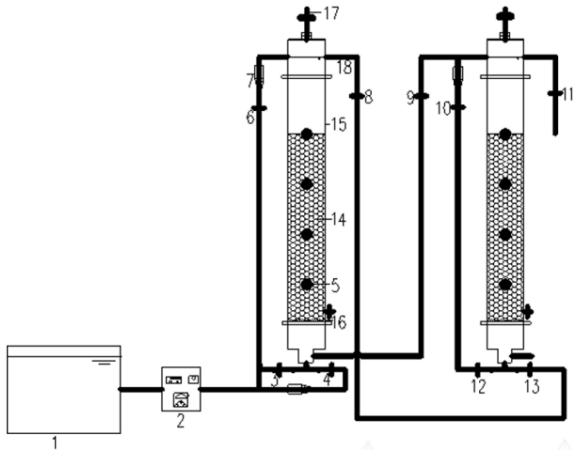


Figure 1. Schematic diagram of the dynamic adsorption experimental setup

Note: 1. Water tank 2. Peristaltic pump 3. Valve 4. Valve 5. Water sampling port 6, 8–13 Valves 7. Flowmeter 14. Modified zeolite 15. Fixed adsorption column 16. Support layer 17. Exhaust port 18. Pipe connection.

Dynamic experiments were conducted in an organic glass column (inner diameter 3 cm, packing height 60 cm, packing amount approximately 200 g). According to the setup in Figure 1, the flow passed through the adsorption column at a velocity of 4 L/h, and the effluent total phosphorus was measured every 1 h until adsorption breakthrough was reached.

3. RESULTS AND DISCUSSION

3.1 Analysis of structural evolution and performance enhancement mechanism of modified zeolite

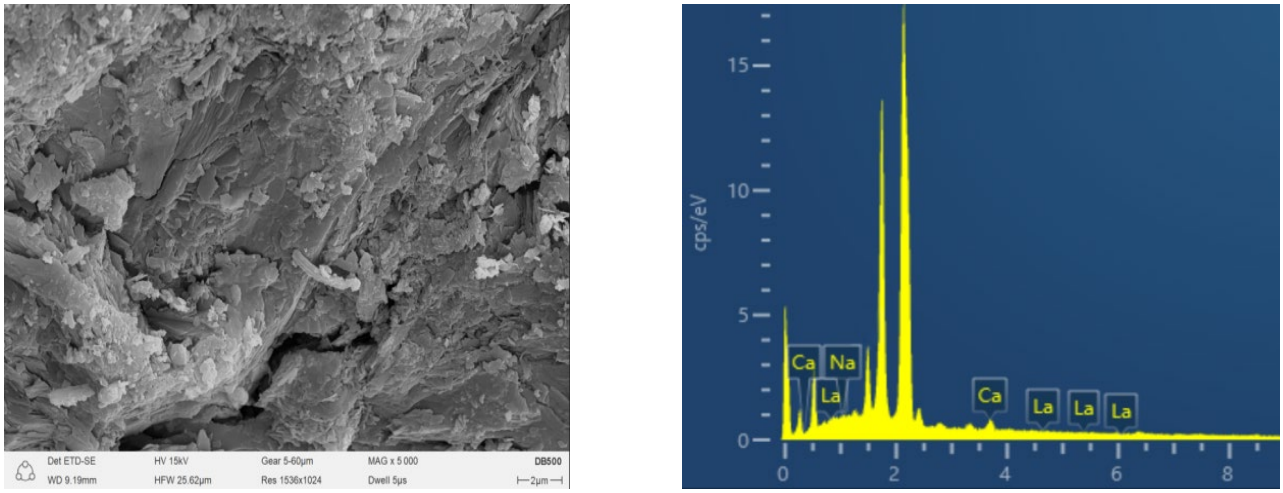
3.1.1 Zeolite phase composition and elemental analysis

As can be seen from the SEM morphology characterization (Figure 2), the zeolite before modification had a flat surface with distinct edges and corners. After lanthanum nitrate treatment, a significant texturing trend appeared on the carrier surface, with a large number of fine particles attached, visually demonstrating the successful loading of lanthanum sites [16]. EDS analysis further revealed the changes in chemical composition: compared with the distribution of Ca (13.52 wt%) and Na (1.88 wt%) before modification, lanthanum could be qualitatively and quantitatively detected after modification, proving the stable immobilization of the active component on the zeolite substrate. This conclusion is

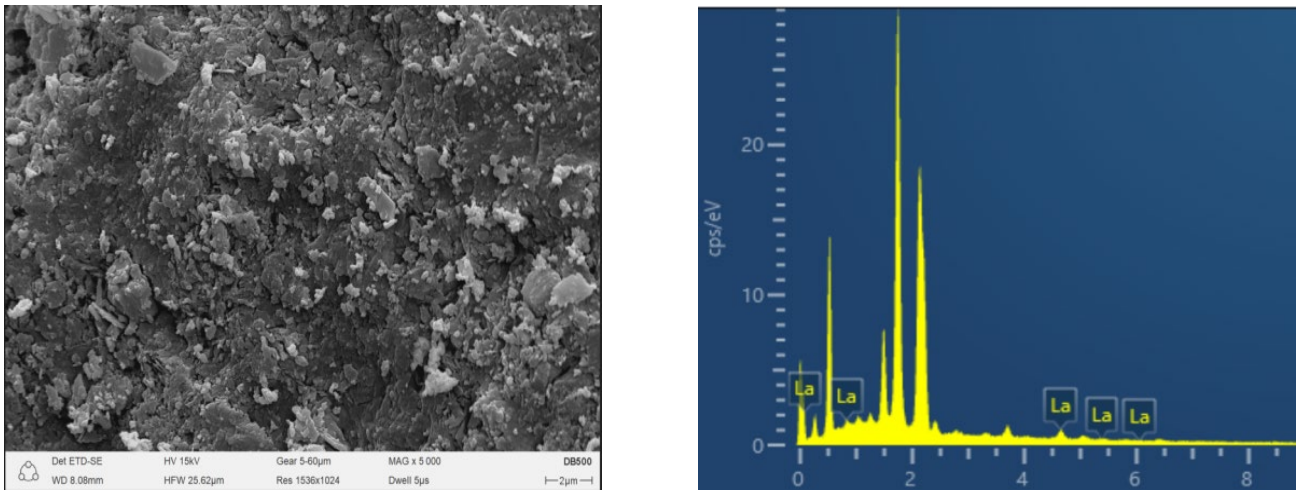
consistent with the pseudo-second-order kinetics and Langmuir thermodynamic model. EDS analysis indicates that La was successfully loaded.

3.1.2 Specific surface area and pore structure analysis

In Table 3, the specific surface area of the zeolite after modification decreased from 13.4655 m^2/g to 9.6880 m^2/g, and the total pore volume decreased from 0.042699 cm^3/g to 0.019728 cm^3/g, indicating that the loading of lanthanum species partially occupied the original pore structure of the zeolite [17, 18]. The t-Plot micropore area increased significantly from 0.1248 m^2/g to 2.4863 m^2/g, the mesoporous cumulative pore volume (Barrett-Joyner-Halenda, BJH) increased from 0.018776 cm^3/g to 0.036788 cm^3/g, while the external surface area decreased from 13.3406 m^2/g to 7.2017 m^2/g. This characteristic of "increased micropores and mesopores, decreased external surface area" is attributed to lanthanum preferentially depositing on the outer surface and mesoporous channels of the zeolite, while simultaneously inducing the formation of new microporous structures inside. Although the specific surface area decreased after modification, the lanthanum loading provided high-affinity specific adsorption sites (Langmuir model) [19], significantly improving the mass transfer efficiency of phosphate, which corresponds to the rapid initial adsorption rate of the pseudo-second-order kinetics (k_2 = 2.35). The essential improvement of lanthanum modification lies in: chemical affinity replacing physical specific surface area as the dominant factor in adsorption.



(a) Characterization via Scanning Electron Microscopy (SEM)–Energy Dispersive Spectroscopy (EDS) image of zeolite before modification



(b) Characterization via Scanning Electron Microscopy (SEM) image of zeolite after modification

Figure 2. Characterization via Scanning Electron Microscopy (SEM)–Energy Dispersive Spectroscopy (EDS) analysis results

Table 3. BET analysis results before and after modification

Sample Name	BET Surface Area (m^2/g)	Langmuir Surface Area (m^2/g)	t-Plot Micropore Area (m^2/g)	t-Plot Micropore Volume (cm^3/g)	Total Pore Volume (cm^3/g)	BJH Adsorption Cumulative Volume (1.7–300 nm) (cm^3/g)
Zeolite before modification	13.4655	21.4495	0.1248	0.000054	0.042699	0.036788
Lanthanum modified zeolite	9.688	14.3632	2.4863	0.00106	0.019728	0.018776

Note: BET = Brunauer–Emmett–Teller; Barrett-Joyner-Halenda = BJH.

3.1.3 X-ray Diffraction results analysis

As shown in the XRD pattern (Figure 3), the zeolite before modification exhibited diffuse broad peaks in the range of 10° to 30°, indicating that its structure was predominantly amorphous with relatively low crystallinity. After lanthanum nitrate modification, the sample showed distinct characteristic diffraction peaks at positions such as 15°, 28°, 30°, and 42°. These peak positions highly coincided with the standard cards of $La(OH)_3$ or La_2O_3 phases, proving that the lanthanum components were successfully loaded on the carrier surface and established crystalline phases [20]. Based on the literature, La is presumed to exist in hydrated/hydroxylated forms. The XRD characterization confirmed the functional morphology of lanthanum active sites from the aspect of phase composition.

3.2 Adsorption isotherm and kinetic analysis of modified zeolite

Comparing the isotherm fitting data in Table 4 and Figure 4, the Langmuir model ($R^2 = 0.9834$) showed a better goodness of fit than the Freundlich model ($R^2 = 0.9261$). The theoretical maximum adsorption capacity (q_m) was 7.94 mg/g, with K_L = 0.149. The phosphorus removal capacity of natural zeolite is generally difficult to exceed 1 mg/g, and the successful loading of lanthanum greatly improved the material performance. The Freundlich constant 1/n = 0.4009 (between 0.1 and 0.5), proving that the adsorption reaction has a good spontaneous tendency and feasibility. Based on the kinetic fitting data in Table 3 and Figure 4, the pseudo-second-order model ($R^2 = 0.9961$) showed a significantly higher goodness of fit than the pseudo-first-order model ($R^2 = 0.9632$). The theoretical equilibrium adsorption capacity ($q_e = 0.0474$ mg/g) was close to the measured value, and its rate constant k_2 was 2.35 g/mg·min. The initial response rate increased significantly [21], and equilibrium could be approached within 60 min.

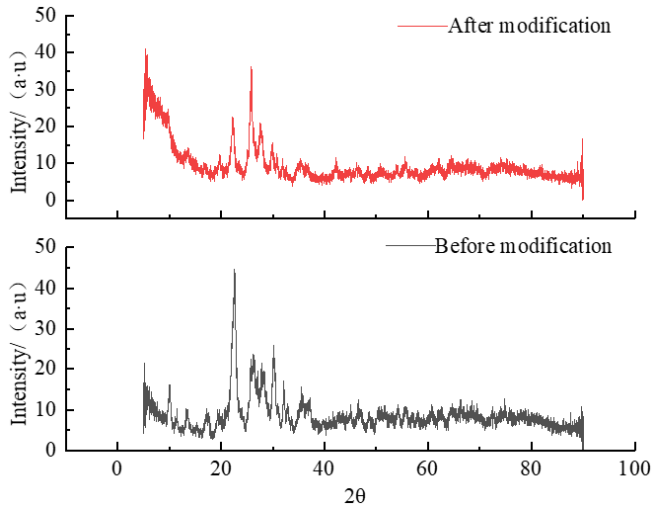
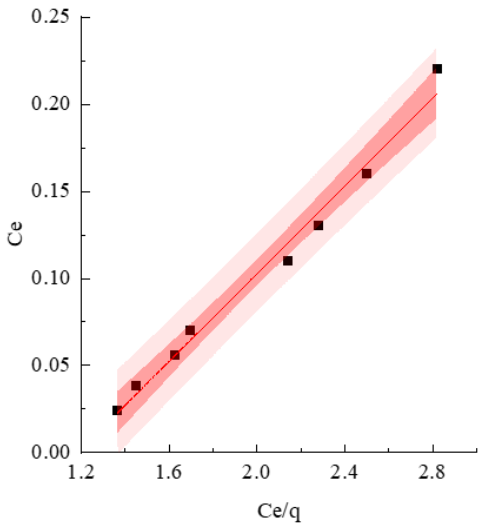


Figure 3. X-ray Diffraction (XRD) pattern analysis

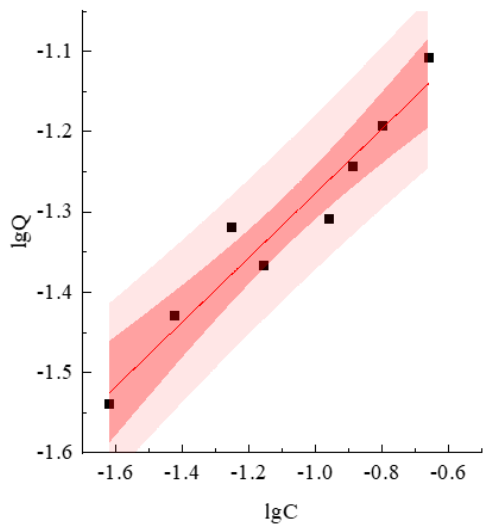
Most of the lanthanum on the zeolite surface exists in the form of hydrated oxide, capturing phosphate through ligand exchange effect, and then forming stable inner-sphere complexes [22, 23]. The essential improvement of lanthanum modification lies in: (1) changing the adsorption driving force from physical electrostatic interaction to coordination covalent bond; (2) introducing specific recognition sites for PO_4^{3-}; (3) changing the adsorption process from diffusion control to chemical reaction control. The synergy of these three aspects endows the modified material with both large adsorption capacity and rapid adsorption kinetics.

Table 4. Adsorption isotherm and adsorption kinetic parameters

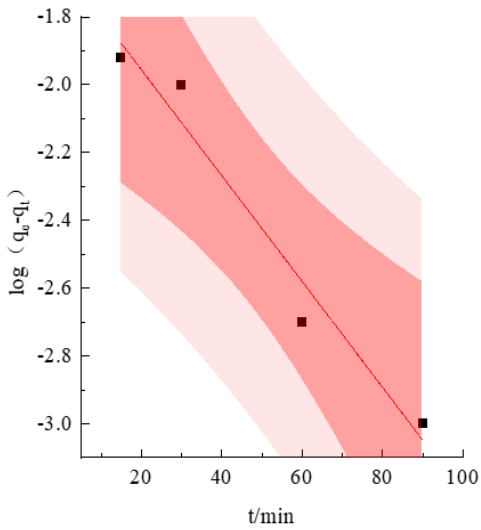
Langmuir Isotherm Adsorption Model				Freundlich Isotherm Adsorption Model			
Fitting Equation	**R^2**	**q_m (mg/g)**	**K_L Adsorption Constant**	**Fitting Equation**	**R^2**	**1/n**	**K_F Adsorption Coefficient**
$y = 0.1259x + 0.019$	0.9834	7.94	0.149	$y = 0.4009x - 0.8757$	0.9261	0.4009	0.133
Pseudo-First-Order Kinetics				**Pseudo-Second-Order Kinetics**			
Fitting Equation	**R_1^2**	**q_{e1} (mg/g)**	**k_{f1} (1/min)**	**Fitting Equation**	**R_2^2**	**q_{e2} (mg/g)**	**k_{f2} (g/mg·min)**
$y = -0.0156x - 1.6443$	0.9632	0.0227	0.0359	$y = 21.106x + 189.28$	0.9961	0.0474	2.35



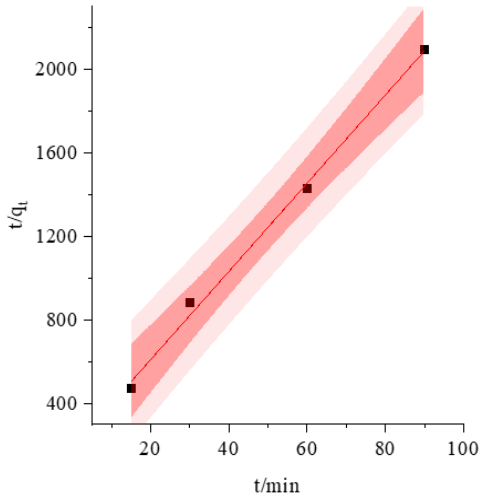
(a) Langmuir adsorption isotherm fitting plot



(b) Freundlich adsorption isotherm fitting plot



(c) Pseudo-first-order kinetics fitting trend line

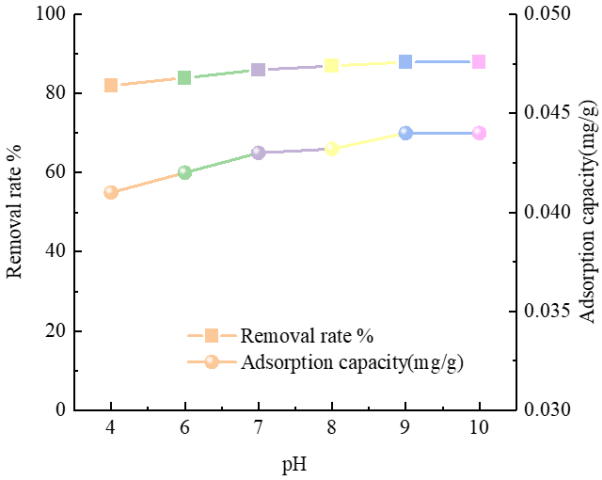


(d) Pseudo-second-order kinetics fitting trend line

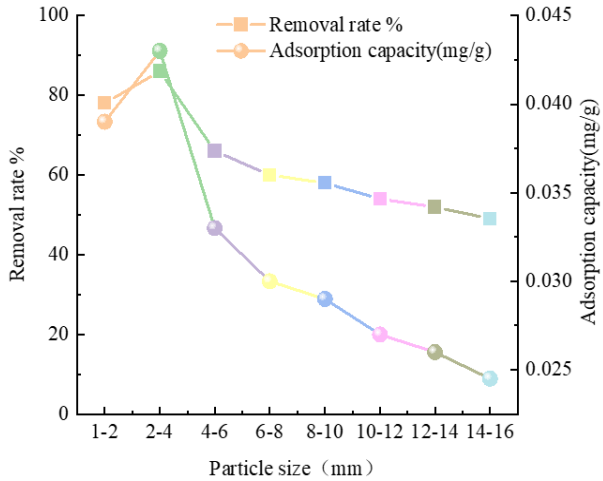
Figure 4. Adsorption isotherm and adsorption kinetic plots

3.3 Adsorption parameter optimization and influence analysis

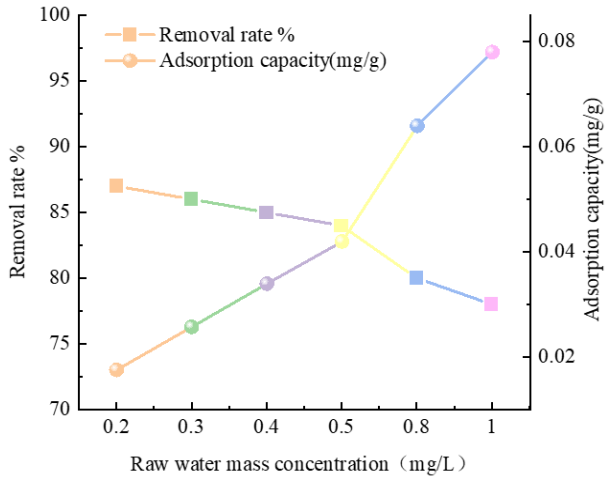
To further determine the phosphorus adsorption behavior of the modified zeolite, a systematic evaluation was conducted on key variables including pH, particle size distribution, initial phosphorus mass concentration, dosage, temperature, and reaction time. The results are shown in Figure 5. The optimal adsorption conditions were: particle size 2–4 mm, dosage 1 g/L, time 60 min, room temperature, pH 7–9, suitable for raw water with total phosphorus mass concentration ≤ 0.5 mg/L, with a removal rate of 85%–89% and adsorption capacity of approximately 0.041–0.043 mg/g.



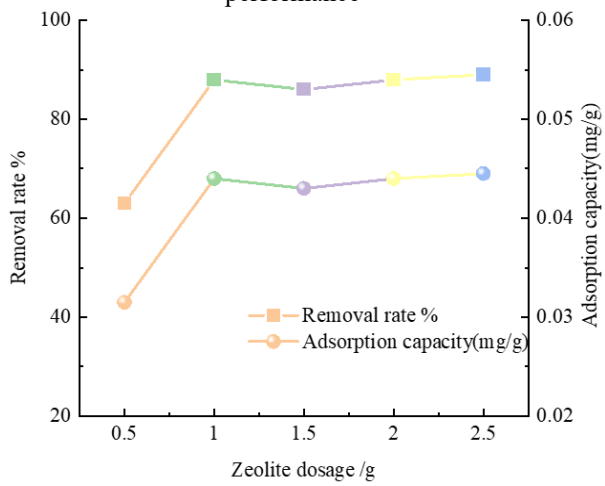
(a) Effect of raw water pH on adsorption performance



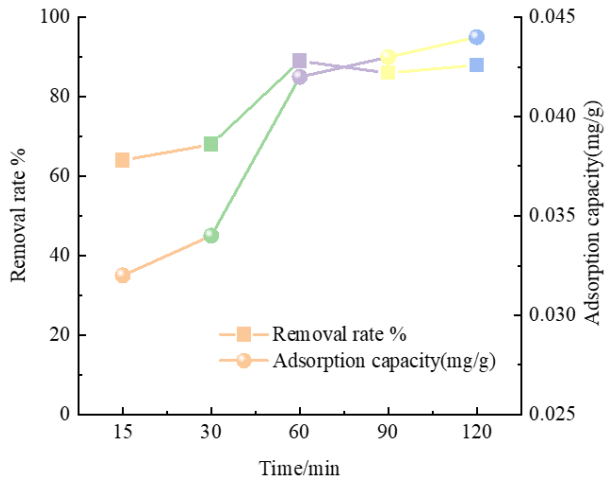
(b) Effect of different particle sizes on adsorption performance



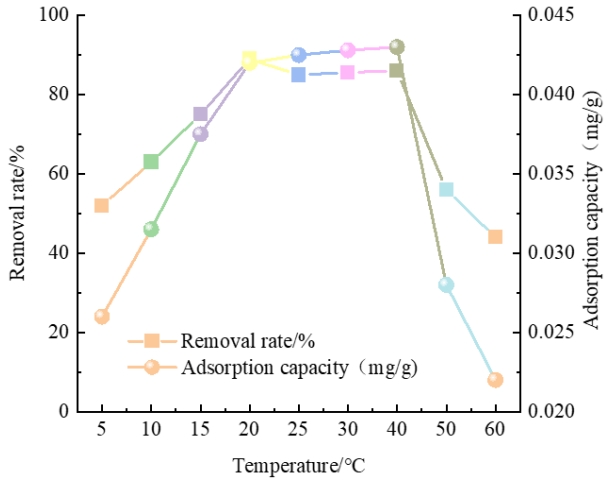
(c) Effect of raw water mass concentration on adsorption performance



(d) Effect of zeolite dosage on adsorption performance



(e) Effect of reaction time on adsorption performance



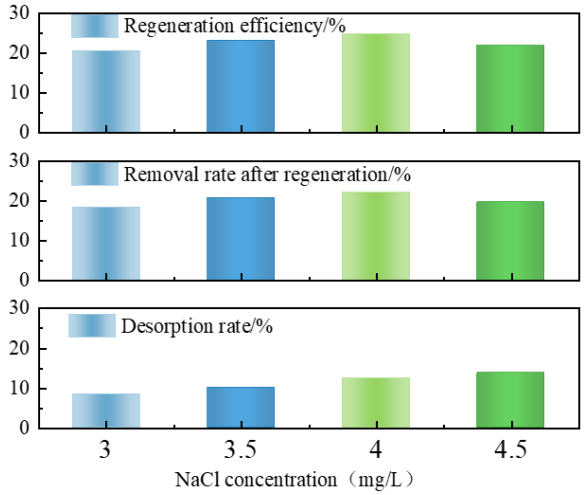
(f) Effect of reaction temperature on adsorption performance

Figure 5. Effect of optimization parameters on adsorption performance

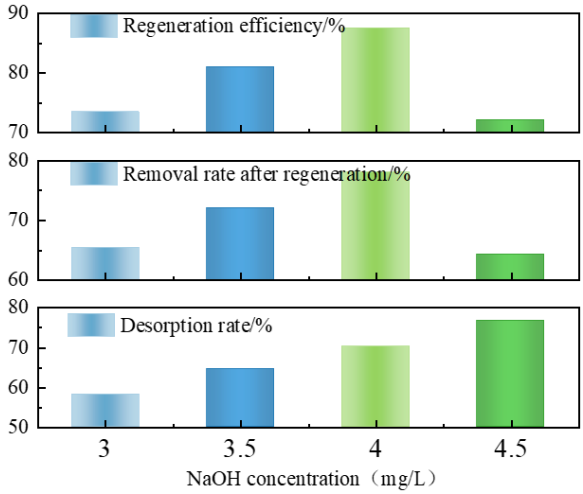
Increasing the particle size (Figure 5(b)) from 2–4 mm to 8–16 mm caused the removal rate to sharply drop from 86% to 52%, mainly due to insufficient effective specific surface area and increased internal diffusion mass transfer resistance. Increasing the dosage (Figure 5(d)) from 0.5 g to 1 g significantly improved the removal rate, but excessive input led to physical agglomeration between particles, reducing the utilization rate of active sites and thus lowering the adsorption efficiency. At initial mass concentrations (Figure 5(c)) ≤ 0.5 mg/L, the results showed good phosphorus removal stability, with the removal rate remaining above 84%. At excessively high concentrations, the saturation effect of adsorption sites reduced treatment efficiency. For adsorption time (Figure 5(e)), there was an instantaneous adsorption in the first 30 min, and equilibrium was rapidly reached within 60 min. The pH (Figure 5(a)) remained stable in the range of 6–10, with the removal rate already above 85% at pH ≥ 7. Considering practical engineering conditions, the optimal pH range was determined to be 7–9. The pH of natural water bodies (7.4–8.6) falls exactly within this range. In alkaline media, phosphate exists mainly as HPO_4^{2-}, and the lanthanum hydrate (La–OH) loaded on the zeolite surface forms stable inner-sphere complexes (La–O–P) with it through ligand exchange, releasing OH^- (La–OH + HPO_4^{2-} → La–O–P + OH^-). At reaction temperatures (f) in the range of 20–40 ℃, the removal rate remained stable at 85%–89%, indicating that room temperature around 20 ℃ can meet the requirements for efficient reaction. Excessively high temperature disturbances would disrupt the integrity of the lanthanum hydrate structure and the stability of the complex products. Considering the actual temperature fluctuation range of natural water bodies and engineering operating costs, room temperature was selected as the operating temperature. These parameters jointly regulate the efficiency and limits of the adsorption process from different dimensions, including physical mass transfer, chemical environment, and reaction kinetics [24]. The adsorption process is dominated by chemical interactions and also exhibits rapid adsorption characteristics [25].

3.4 Desorption performance and reuse stability experimental analysis

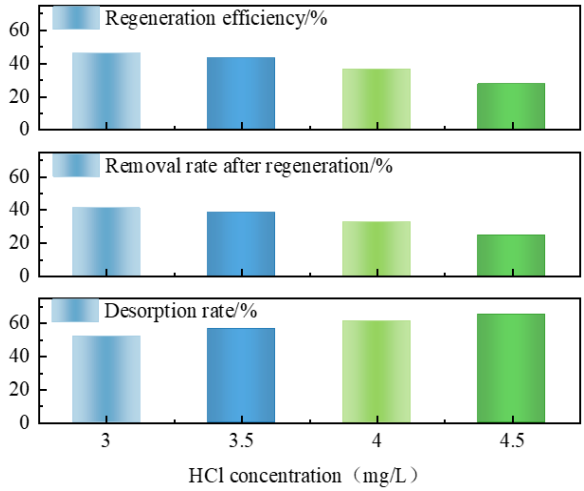
To evaluate the disposal method, reuse potential, and secondary pollution risk of the modified zeolite after adsorption saturation, relevant experimental studies were conducted. The desorption and regeneration tests showed in Figure 6: NaOH had the best desorption effect, followed by HCl, and NaCl was the worst. NaCl relied on relatively weak ion exchange, resulting in the poorest performance.



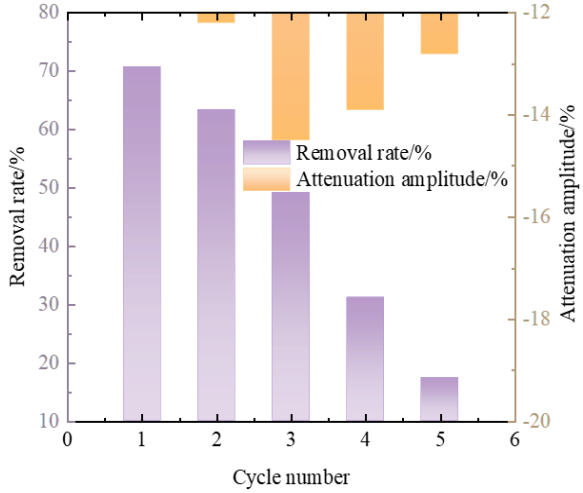
(a) Effect of NaCl concentration on regeneration performance



(b) Effect of NaOH concentration on regeneration performance



(c) Effect of HCl concentration on regeneration performance



(d) Removal rate and attenuation trend over five adsorption–regeneration cycles

Figure 6. Effects of different desorbents concentration on regeneration efficiency and adsorption-regeneration cycle performance

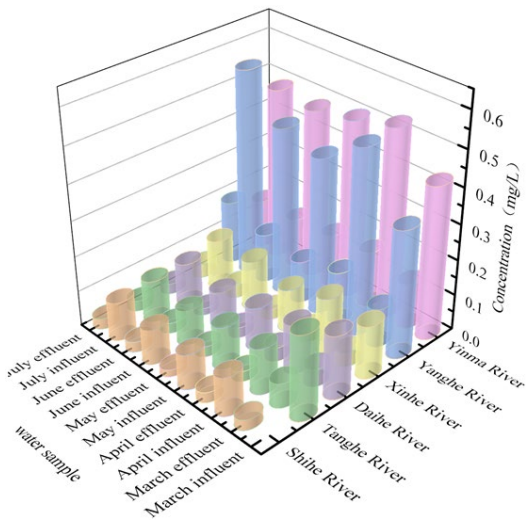
Note: Regeneration efficiency η = removal rate after regeneration / raw material removal rate (89%) × 100%; Desorption rate De = amount of phosphorus desorbed / amount of phosphorus adsorbed × 100%.

Mechanistically, OH^- can competitively break the La–P inner-sphere coordination bond to achieve phosphorus desorption, while H^+ can only dissociate electrostatically adsorbed phosphorus and has difficulty decomposing stable complexes. During the cycling test (Figure 6(d)), the phosphorus removal rate dropped from 71% in the first cycle to below 20% in the fifth cycle. This was mainly controlled by factors such as irreversible occupation of active sites, lanthanum loss caused by repeated acid–base treatment, and physical damage to the microporous structure. The study found that the alkali regeneration mode can reduce solid waste pressure and achieve phosphorus recovery to some extent, and the risk of lanthanum leaching under conventional operation is relatively low. In contrast, if the saturated adsorbent is directly landfilled, there is a potential environmental risk of trace lanthanum leaching and phosphorus re-release due to long-term leaching, but direct landfill of saturated material carries the risk of lanthanum leaching and phosphorus re-release caused by long-term leaching.

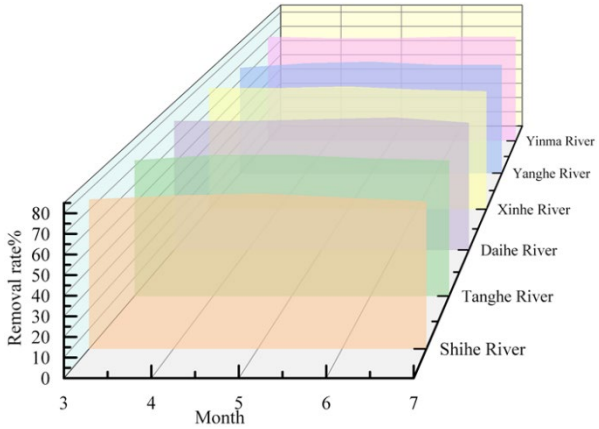
3.5 Total phosphorus removal application of modified zeolite in actual rivers discharging into the sea

Six typical rivers discharging into the sea in the Qinhuangdao area (Shihe River, Tanghe River, Daihe River, Yanghe River, Yinma River, and Xinhe River) were selected for practical application tests. The pH of the water samples from each river ranged from 7.86 to 8.90, which falls within the suitable adsorption range of the modified zeolite.

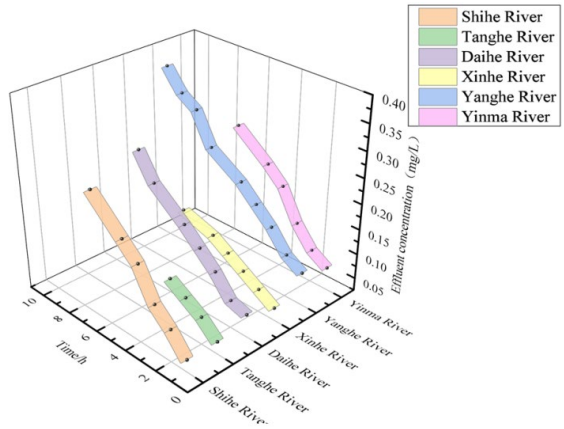
In static tests (Figure 7(a) and (b)), the average removal rate of modified zeolite for the six river water samples was 73.3%, and the effluent total phosphorus was reduced to 0.021–0.175 mg/L, all meeting the Surface Water Class III standard (≤0.2 mg/L). Four of them met the Class II standard (≤0.1 mg/L), with a standard deviation of parallel experiments less than 1.6%. The dynamic breakthrough curve Figure 7(c) showed that: for low-concentration rivers (C_0 = 0.12–0.15 mg/L), the effluent total phosphorus was always below 0.13 mg/L, with a removal rate >75% and a flat curve; for medium-concentration rivers (C_0 = 0.28–0.29 mg/L), the removal rate was 55%–76% in the first 5 h; for high-concentration rivers (C_0 = 0.37 mg/L), breakthrough was approached after 7 h. Both modes followed the pattern of "high removal rate at low concentration, low removal rate at high concentration," which is consistent with the Langmuir model. The initial dynamic removal rate (55%–76%) was lower than the static rate (70%–76%) because the liquid–solid contact time was limited (approximately 2.1 min), and some active sites within the pores had not yet reached saturation. Compared with simulated water, competing anions (SO_4^{2-}, HCO_3^-, etc.) and natural organic matter in natural water bodies competitively occupied the lanthanum active sites, significantly shortening the breakthrough time in actual water bodies (the high-concentration Yanghe River reached breakthrough in only 7 h). Under low-concentration conditions (C_0 < 0.2 mg/L), the modified zeolite still achieved a removal rate >75%, and the effluent quality met the Surface Water Class III standard, indicating that it has good phosphorus removal performance and operational stability in micro-polluted water bodies. Under low concentration (C_0 < 0.2 mg/L), the removal rate was >75%, and the effluent met the Class III standard, indicating its potential for engineering applications.



(a) Total phosphorus concentration of influent and effluent in static adsorption



(b) Total phosphorus removal rate of static adsorption for actual water bodies



(c) Dynamic adsorption breakthrough curve of actual water bodies

Figure 7. Phosphate removal performance of lanthanum-modified zeolite for actual water samples from the main rivers in Qinhuangdao

3.6 Economic analysis

Based on the optimized process parameters from laboratory experiments, a preliminary calculation of the preparation cost of lanthanum nitrate modified zeolite and the water treatment cost was conducted (main raw material prices were estimated at market average prices, excluding labor and equipment depreciation). The results are shown in Table 5.

Table 5. Cost estimation for preparation of modified zeolite and water treatment

Cost Item	Consumption	Unit Price (yuan)	Subtotal (yuan)
Natural zeolite	1.0 t	700/t	700
Lanthanum nitrate	0.10 t	8,500/t	850
Water and electricity	—	—	180
Total (per ton of modified zeolite)			≈1,730
Water treatment chemical cost (dosage 10 g/L)	10 kg/t water	1.73 Yuan/kg	≈17.3 Yuan/t water
NaOH regeneration cost (averaged over 5 cycles)	—	—	≈0.2 Yuan/t water

Note: Lanthanum nitrate is calculated based on an impregnation concentration of 10 g/L and a solid–liquid ratio of 1:10. In actual production, the impregnation solution can be recycled, further reducing the cost.

Under the optimal adsorption conditions (dosage 10 g/L, treating raw water with total phosphorus ≤ 0.5 mg·L^{-1}, removal rate 85%–89%), the material cost for treating 1 ton of water is approximately 17.3 yuan. After 5 cycles of regeneration, the regeneration chemical cost is approximately 3.46 yuan/t water, and the unit treatment cost further decreases with increasing cycle number. Compared with commercial lanthanum-based phosphorus-locking agents (approximately 20,000–30,000 yuan/ton), this material has a significant raw material cost advantage. Compared with conventional coagulation methods, although this material requires a relatively larger initial dosage, it has advantages such as recyclability and regeneration, no secondary pollution, and phosphorus resource recovery potential. The preparation cost of lanthanum nitrate modified zeolite is approximately 1,730 yuan/ton, corresponding to a unit water treatment chemical cost of approximately 1.73 yuan/ton water. Combined with its good regeneration performance, it has good economic feasibility for low-concentration phosphorus pollution treatment in rivers discharging into the sea. It should be noted that the risks of La leaching and phosphorus re-release during long-term use still need to be further evaluated.

4. CONCLUSIONS

(1) XRD, SEM-EDS, and BET indicate that La was successfully loaded and that the pore structure was altered. XRD supports the presence of $La(OH)_3$/La_2O_3 crystalline phases, suggesting that La exists in hydrated/hydroxylated forms. Ligand exchange is considered the main mechanism. A micro-mesoporous hierarchical structure was formed, and this hierarchical pore system effectively reduces mass transfer resistance, which is consistent with the fast adsorption kinetics.

(2) In terms of fitting of thermodynamic and kinetic models, the Langmuir model and pseudo-second-order kinetics showed high adaptability, confirming that the adsorption is monolayer chemical adsorption. After lanthanum modification, the physicochemical properties of the zeolite were well optimized, with a theoretical maximum adsorption capacity of 7.94 mg/g. The adsorption mechanism changed from physical diffusion to chemical reaction rate control.

(3) The optimal phosphorus removal conditions for lanthanum nitrate modified zeolite are: particle size 2–4 mm, dosage 1 g/L, time 60 min, room temperature, pH 7–9. It is suitable for raw water with TP ≤ 0.5 mg/L, with a removal rate of 85%–89%. The driving force changed from physical electrostatic interaction to coordination bond dominated by ligand exchange, overcoming the limitation of natural materials' adsorption failure in near-neutral water bodies.

(4) Field validation on six rivers discharging into the sea in Qinhuangdao showed that the static phosphorus removal rate of the modified zeolite remained stable at an average of 73.3%, and the effluent total phosphorus met the Surface Water Class III standard. In dynamic continuous flow tests, the interception

rate remained above 75% under low phosphorus load, with a smooth breakthrough curve, showing robust phosphorus removal resistance under complex background. Lanthanum modification significantly improved the adsorption performance and water quality compatibility of zeolite through driving force enhancement, specific site anchoring, and pore structure optimization, providing a key technical path for the standard-reaching treatment of low-concentration phosphorus pollution (≤0.5 mg/L) in rivers discharging into the sea.

FUNDINGS

This paper was supported by Science Research Project of Hebei Education Department (Grant No.: QN2025388) and School-level Scientific Research Project of Hebei University of Environmental Engineering (Grant No.: XJXM-YB-2024005).

REFERENCES

[1] Correll, D.L. (1998). The role of phosphorus in the eutrophication of receiving waters: A review. Journal of Environmental Quality, 27(2): 261-266. https://doi.org/10.2134/jeq1998.00472425002700020004x

[2] Cao, X.H., Yu, Z.M., Song, X.X., Yuan, Y.Q., Wu, Z.X., He, L.Y. (2017). Pollution and discharge from tributaries to the sea along Qinhuangdao coast: Impact on the bioactive elements related to brown tide outbreak. Oceanologia et Limnologia Sinica, 48(5): 970-981. https://doi.org/10.11693/hyhz20170300077

[3] Wu, Y.M., Tu, X., Wu, L.X., Guo, Y.T., Li, K., Deng, M. (2024). Experimental study on removal of ammonia nitrogen and total phosphorus from municipal sewage by artificial zeolite and polymerized ferrous sulfate. Technology of Water Treatment, 50(8): 81-86. https://doi.org/10.16796/j.cnki.1000-3770.2024.08.014

[4] Wu, M.M., Song, J.Y., Ma, P.Z., et al. (2021). Study on characteristics of phosphorus adsorption by natural zeolite. Applied Chemical Industry, 50(z2): 124-129. https://doi.org 10.3969/j.issn.1671-3206.2021.z2.026

[5] Luo, Q.Y., Wei, J., Guo, Z., Song, Y.H. (2024). Adsorption and immobilization of phosphorus from water and sediments using a lanthanum-modified natural zeolite: Performance, mechanism and effect. Separation and Purification Technology, 329: 125187. https://doi.org/10.1016/j.seppur.2023.125187

[6] Chen, B.B., Tang, Y., He, D.S., et al. (2023). Phosphorus adsorption properties in waste water of La− modified synthetic zeolite from coal fly ash. Conservation and Utilization of Mineral Resources, 43(3): 152-159. https://doi.org/10.13779/j.cnki.issn1001-0076.2023.03.018

[7] Li, X.D., Kuang, Y., Chen, J.B., Wu, D.Y. (2020). Competitive adsorption of phosphate and dissolved organic carbon on lanthanum modified zeolite. Journal of Colloid and Interface Science, 574: 197-206. https://doi.org/10.1016/j.jcis.2020.04.050

[8] Pham, T.H., Lee, K.M., Kim, M.S., Seo, J., Lee, C. (2019). La-modified ZSM-5 zeolite beads for enhancement in removal and recovery of phosphate. Microporous and Mesoporous Materials, 279: 37-44. https://doi.org/10.1016/j.micromeso.2018.12.017

[9] Fang, Z., Liu, W.D., Xue, N., Yang, K., Zhang, Z.H. (2016). Zeolite modified and de-fluorination performance in zinc sulfate solution. Nonferrous Metals Science and Engineering, 7(6): 88-93. https://doi.org/10.13264/j.cnki.ysjskx.2016.06.015

[10] Freundlich, H. (1907). Over the adsorption in solution. Journal of Physical Chemistry, 57(1): 385-470. https://doi.org/10.1515/zpch-1907-5723

[11] Langmuir, I. (1918). The adsorption of gases on plane surfaces of glass, mica and platinum. Journal of the American Chemical Society, 40(9): 1361-1403. https://doi.org/10.1021/ja02242a004

[12] Ezzati, R., Ezzati, S., Azizi, M. (2024). Exact solution of the Langmuir rate equation: New insights into pseudo-first-order and pseudo-second-order kinetics models for adsorption. Vacuum, 220: 112790. https://doi.org/10.1016/j.vacuum.2023.112790

[13] Sutherland, C. (2025). A method of classifying the influence of intraparticle diffusion in adsorption systems: Characteristic curves of the diffusion-chemisorption kinetic model. Environmental Toxicology and Chemistry, 44(5): 1209-1221. https://doi.org/10.1093/etojnl/vgaf052

[14] Fang, L.Y., Hu, Y.Y., Han, R.P., Qu, L.B. (2026). Adsorption of fluoride and phosphate by manganese and aluminum-loaded magnetic Fe_3O_4 in batch mode. ChemistrySelect, 11(13): e02665. https://doi.org/10.1002/slct.202502665

[15] Liu, Z.P., Chen, J.C., Song, C., et al. (2024). Measurement uncertainty assessment of ammonium molybdate spectrophotometric determination of total phosphorus content in fishery water. Chinese Fishery Quality and Standards, 14(3): 8-15. https://doi.org/10.3969/j.issn.2095-1833.2024.03.002

[16] Lai, Y.Q., Yang, K., Yang, C., Tian, Z.L., Guo, W.C., Li, J. (2018). Thermodynamics and kinetics of fluoride removal from simulated zinc sulfate solution by La(III)-modified zeolite. Transactions of Nonferrous Metals Society of China, 28(4): 783-793. https://doi.org/10.1016/S1003-6326(18)64711-9

[17] He, Y.H., Lin, H., Dong, Y.B., Wang, L. (2017). Preferable adsorption of phosphate using lanthanum-incorporated porous zeolite: Characteristics and mechanism. Applied Surface Science, 426: 995-1004. https://doi.org/10.1016/j.apsusc.2017.07.272

[18] Lu, Y.Y., Wang, H., Chang, R.R., Li, W.B., Huang, B.C., Jin, R.C. (2024). A literature review on phosphate removal from wastewater by lanthanum-based adsorbents: From mechanisms to applications. Journal of Water Process Engineering, 59: 105282. https://doi.org/10.1016/j.jwpe.2024.105282

[19] Li, Y.Z., Shen, Z.Q., Zhou, Y.X., Zhou, J.H., Liu, J. (2014). Study on quick adsorption characteristics of ammonia on natural clinoptilolite. Journal of Environmental Engineering Technology, 4(4): 275-281. https://doi.org/10.3969/j.issn.1674-991X.2014.04.045

[20] Zhang, W.K., Tian, Y. (2015). Phosphorous removal from wastewater by lanthanum modified Y zeolites. Frontiers of Chemical Science and Engineering, 9: 209-215. https://doi.org/10.1007/s11705-014-1448-4

[21] Pan, M., Zhang, M.C., Zou, X.H., et al. (2019). The investigation into the adsorption removal of ammonium by natural and modified zeolites: Kinetics, isotherms,

and thermodynamics. Water SA, 45(4): 648-656. https://doi.org/10.17159/wsa/2019.v45.i4.7546
[22] Luo, Q.Y., Zhang, X.D., Wei, J., Zhang, J.L., Guo, Z., Song, Y.H. (2025). High-efficiency lanthanum-modified zeolite adsorbents for phosphorus control and algal suppression: Preparation, characterization and mechanistic insights. Separation and Purification Technology, 352: 128146. https://doi.org/10.1016/j.seppur.2024.128146
[23] Zhou, B.L., Zhang, C.Y., Li, Z.G., Li, C.H. (2020). Study on synergistic effect of removal of nitrogen and phosphorus by mixed modified zeolite. IOP Conference Series: Earth and Environmental Science, 508: 012156. https://doi.org/10.1088/1755-1315/508/1/012156
[24] Zhang, D.F., Shi, C.B., Xu, Z.H. (2011). Experiment on micro-polluted water by biological treatment of natural zeolite and peat. Journal of Water Resources and Water Engineering, 22(2): 1-4. https://doi.org/10.11705/j.issn.1672-643X.2011.02.045
[25] Lin, J.W., Wang, H., Zhan, Y.H., Chen, D.M. (2016). Adsorption of phosphate by lanthanum hydroxide/natural zeolite composites from low concentration phosphate solution. Environmental Science, 37(1): 208-219. https://doi.org/10.13227/j.hjkx.2016.01.028